World Academy of Science, Engineering and Technology
International Journal of Mechanical and Mechatronics Engineering
Vol:6, No:2, 2012

Fatigue Life of an Anti-Roll Bar of a Passenger Vehicle

J. Marzbanrad, A. Yadollahi

***Abstract*—**In the present paper, Fatigue life assessment of an anti-roll bar component of a passenger vehicle, is investigated by ANSYS 11 software. A stress analysis is also carried out by the finite element technique for the determination of highly stressed regions on the bar. Anti-roll bar is a suspension element used at the front, rear, or at both ends of a car that reduces body roll by resisting any unequal vertical motion between the pair of wheels to which it is connected. As a first stage, fatigue damage models proposed by some well-known references and the corresponding assumptions are discussed and some enhancements are proposed. Then, fracture analysis of an anti-roll bar of an automobile is carried out. The analysed type of the anti-roll bar is especially important as many cases are reported about the fracture after a 100,000 km of travel fatigue and fracture conditions. This paper demonstrates fatigue life of an anti-roll bar and then evaluated by experimental analytically results from other researcher.

***Keywords*—**Anti-roll bar, Fracture, Fatigue life, Random loading

I. Introduction

GROUND vehicle design typically represents a trade-off between performance and safety. Design parameters affecting lateral dynamics can influence maneuvering ability, but also have some influence on the dynamic stability including spinout and rollover. In steering maneuvers, vertical loads on tires at the outer track increase and those on the inner track decrease, which is called lateral load transfer. When moment equilibrium is broken at some conditions, a vehicle loses roll stability. Geometric dimensions, suspension characteristics as well as maneuvering conditions influence the dynamic roll behavior of a car. To improve the roll characteristics of a car, the customary approach is to increase the roll stiffness by using a stabilizer bar which affects the ride comfort with respect to high frequency isolation induced by road excitation. In order to enhance the vehicle performance, several experiences are studied. At present one of the most efficient methods is the roll control with a semi-active suspension system in order to isolate the driver from roadway noise, road holding on irregular road surfaces and safe turning through steering. As is the case with any vehicle system, an actual car is expected to operate in a highly variable environment. For instance, parameter variations resulting from loading pattern and driving condition will influence vehicle dynamics [1].

The antiroll bar is a circular sectioned torsion bar mounted transversely on spaced out rubber bush swivel bearings to the body and having cranked arms.

J. Marzbanrad is with the Iran University of Science and Technology, School of Automotive Engineering, Iran, Tehran (phone: 9821-7720360; fax: 9821-77491224; e-mail: marzban@ iust.ac.ir).

A. Yadollahi is with the Islamic Azad University, Semnan Branch, Automotive Department, Iran, Semnan (e-mail: aref_yaollahi@auto.iust.ac.ir).

That is, bent extended ends which are attached to each swing-arm via short vertical link-rods by means of rubber-bush joints. Thus the function of the antiroll bar is to relieve the main suspension springs of some of their load every time the body rolls. An antiroll bar stiffens the suspension springing when the body rolls or one wheel goes over a bump or dip in the road. The antiroll bar therefore permits softer suspension springing to be used when the vehicle is moving straight ahead, as this responds far better than hard springing to small ripples or irregularities in the road, hence it improves the ride comfort of the passengers. In the extreme, some antiroll bars are tuned to take as much as 30–40% of the total vertical load imposed on the suspension when subjected to severe body roll [2]. Fig. 1, shows the anti-roll bar in case of the installation. The anti-roll bar picture analysed in this study is given in Fig. 2.Recently many cases of fractured anti-roll bars after a 100,000 km of travel for a special passenger car are reported. All of the bars are fractured at nearly the same location (Fig. 3). In this study, fracture analysis of this anti-roll bar is carried out. Mechanical characteristics of the material are obtained first. Then the microstructure and chemical compositions are determined. Some fractographic studies are carried out to access the fatigue and fracture conditions. A stress analysis is also carried out by the finite element technique for the determination of highly stressed regions on the bar.Many engineering components are subjected to complex combinations of loads that fluctuate with time in a non-proportional manner. In some cases, time variations of the loads are of random nature. Component that are used in airplanes, ground vehicles, marine and offshore structures, railways, and bridges are subjected to loads that vary with time in a very complicated manner. Many fatigue damage models have been proposed in the literature, most of them are limited to specific materials or simple loading conditions. Multiaxial fatigue criteria are presented based on different concepts: stress invariants, energy, critical plane, fracture mechanics, etc. Fatigue damage increases with the number of cycles of the applied load in a cumulative manner. Many cumulative damage theories are reviewed by Fatemi and Yang [3]. A theory is proposed in the present paper that is suitable for life assessment in three-dimensional stress fields. Generally, the aim of the fatigue damage models proposed so far was checking the fatigue failure strength rather than calculating the number of cycles or number of history blocks that may lead to the fatigue failure. In the current paper, an algorithm is developed to predict the fatigue life based on the damage models that are proposed in the paper. Result obtained based on FEM analysis by ANSYS 11 software is compared with some well-known damage theories, the modified theories and the experimental results prepared by another author.

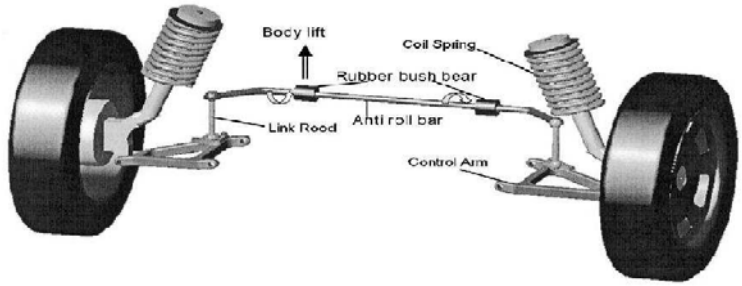

Fig. 1 Schematic presentation of an anti-roll in action

Fig. 2 The picture of the undamaged anti-roll bar analysed in this study

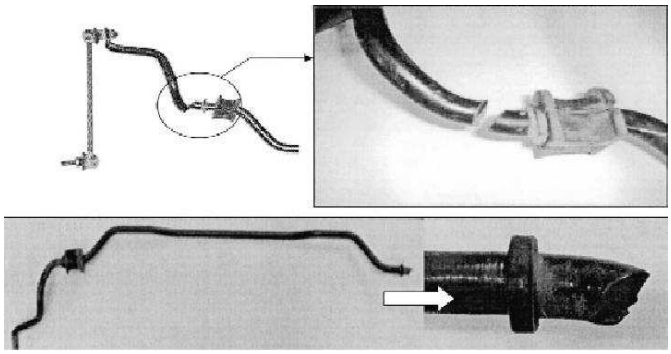

Fig. 3 Two different fractured anti-roll bar

II. Fatigue Assessment Criteria

Stress-based multi-axial fatigue failure criteria have already been developed based on experimental observations. Some of these criteria as well as some recently proposed criteria are mentioned in the current section.

A. Von Mises and Tresca criteria

The analytical forms of these criteria are respectively [4]:

Tresca criterion:

$$\sqrt{J_2}\sin(\alpha+\pi/3)\tau_f,\quad \alpha=\frac{1}{3}\cos^{-1}\left(\frac{3\sqrt{3}.J_3}{2J_2^{3/2}}\right):-\frac{\pi}{6}<\alpha<\frac{\pi}{6} \tag{1}$$

Von Mises criterion:

$$J_2=\frac{1}{6}\left[(\sigma_1-\sigma_2)^2+(\sigma_2-\sigma_3)^2+(\sigma_3-\sigma_1)^2\right]=\sigma_f^3/3 \tag{2}$$

where J_2 and J_3 are the second and the third invariants of the deviatoric stress tensor, respectively, σ_1, σ_2, and σ_3 are the principal stresses, and τ_f and σ_f are the fatigue failure stresses. In many applications, the stress state can be reduced to a two-dimensional state including a normal stress and a shear stress components only (e.g. for a component under combined bending and torsion). In these situations, (1), can be rewritten as:

$$\sqrt{\sigma_{\max}+(\varphi\tau_{\max})^2}=\sigma_f \tag{3}$$

where the value of φ is 2 and $\sqrt{3}$ for Tresca and Von- Mises criteria, respectively.

B. Ellipse quadrant criterion

Gough and pollard, proposed the following modified von Mises criterion for in-phase fully reversed loadings [12]:

$$\left(\frac{\sigma_a}{\sigma_{R=-1}}\right)^2+\left(\frac{\tau_a}{\tau_{R=-1}}\right)^2=1 \quad (4)$$

where $\sigma_{R=-1}$ and $\tau_{R=-1}$ are the fatigue strength values for the specified number of cycles to failure. In the present paper, the following abbreviations are used, for simplicity:

$$\sigma_R \equiv (\sigma_a)_R, \tau_R \equiv (\tau_a)_R \quad (5)$$

C. Sines criterion [5]

Sines suggested that fatigue failure is achieved when the following condition is satisfied [6]:

$$\sqrt{(J_2)_a}+\alpha(I_1)_m=\beta$$
$$\alpha=(3\tau_{R=-1}-\sqrt{3}\sigma_{R=-1})/\sigma_m\beta+\tau_{R=-1} \quad (6)$$

$I_1=\sigma_h$ is the first stress invariant (σ_h is the hydrostatic stress) and α and beta are material parameters.

D. Findley criterion

Findley criterion may be described as [7]:

$$(\tau_a+k\sigma_n)_{\max(\theta,\psi,\varphi)}=f$$
$$k=\frac{2-\sigma_{R=-1}/\tau_{R=-1}}{2\sqrt{\sigma_{R=-1}/\tau_{R=-1}-1}} \quad (7)$$
$$f=\sqrt{\frac{(\sigma_{R=-1})^2}{4\sqrt{\sigma_{R=-1}/\tau_{R=-1}-1}}}$$

According to this criterion, the critical plane is a plane where $\max_{\theta,\varphi,\psi,t}(\tau_a+k\sigma_n)$ occurs θ, φ, and ψ are the Eulerian angles and t denotes the time.

E. McDiarmid criterion

McDiarmid used the concept of type A and type B cracks introduced by Brown and Miller [8] to develop his linear criterion:

$$\tau_a+k(\sigma_a)_{\max(t)}=f$$
$$k=(\tau_f)_{AorB}/2\sigma_u \quad (8)$$
$$f=(\tau_f)_{AorB}$$

where σ_u is the ultimate strenght. According to this criterion, at the critical plane $\max_{\theta,\varphi,\psi,t}(\tau_a)$ is achieved. Therefore, two limit cases (upper and lower limits) are predicted.

F. Carpinteri–Spagnoli theory

Carpinteri and Spagnoli proposed the following nonlinear relationships to be evaluated to determine the critical plane [9-11]:

$$\left(\frac{\tau_a}{\tau_{R=-1}}\right)^2+\left(\frac{\sigma_{n,\max}}{\sigma_{R=-1}}\right)^2=1 \quad (9)$$

The weighted mean principal stress method is used to determine the critical plane.

G. Ninic criterion

Ninic [12] has presented a criterion that modifies Gough's criterion as follows:

$$\left(\frac{\tau_a}{\tau_{R=-1}}\right)^2+k\left(\frac{\sigma_a+\sigma_{R=-1}(\sigma_m/\sigma_n)^2}{\sigma_{R=-1}}\right)^2=1 \quad (10)$$

where *k* is a normal stress sensitivity factor that is calculated based on a maximization procedure, as:

$$k=\begin{cases}\left(\frac{\sigma_{R=-1}}{\tau_{R=-1}}\right)^2\left[1-\left(\frac{\sigma_{R=-1}}{2\tau_{R=-1}}\right)^2\right] & 0\le\frac{\tau_{R=-1}}{\sigma_{R=-1}}\le\frac{\sqrt{2}}{2}\\ 1 & \frac{\sqrt{2}}{2}\le\frac{\tau_{R=-1}}{\sigma_{R=-1}}\end{cases} \quad (11)$$

H. Liu criterion

Liu et al. [13] proposed the following characteristic plane based criterion:

$$\left[\frac{\sigma_a(1+\eta\frac{\sigma_m}{\sigma_{R=-1}}}{\sigma_{R=-1}}\right]^2+\left(\frac{\tau_a}{\tau_{R=-1}}\right)^2+k\left(\frac{\sigma_a^H}{\sigma_{R=-1}}\right)^2=\mu \quad (12)$$

where σ_a^H is the hydrostatic stress amplitude. This criterion may be considered as a modified version of Gough's criterion. The main aim was to substitute the 3D stress field variation effect by the effect of the amplitude value of the normal and the shear stresses acting on a characteristic plane, considering the time variation of the hydrostatic stress amplitude.

I. Von Mises and Tresca criteria

Tresca and Von Mises criteria, (1) and (2), are suitable for proportional fully reversed loadings. Although the effect of the mean shear stress is often neglected in HCF analysis [18], Goodman and Gerber curves reveal that the shear mean stress effect may be accounted for. Fatigue damage of a normal uni-axial stress that varies with a mean value σ_m and an amplitude σ_R is related through the following equations to the fully reversed one with the same fatigue damage:

Modified Goodman line equation:

$$\sigma_R = \begin{cases} \sigma_{R=-1}\left(1-\dfrac{\sigma_m}{\sigma_R}\right) & 0 \le \sigma_m \\ \sigma_{R=-1} & \sigma_m \le \sigma_R \end{cases} \tag{13}$$

Gerber equation:

$$\sigma_R = \sigma_{R=-1}[1-(\sigma_m/\sigma_u)^2] \tag{14}$$

Similar equations can be written for the shear stress. Test results tend to fall between Goodman and Gerber curves. The material parameter φ appeared in (3), may be calibrated using results of the pure bending (or pure tension) and pure torsion fatigue experiments. Therefore, one may write:

$$\left(\frac{\tau_{\max}}{\tau_m+\tau_R}\right)^2+\left(\frac{\sigma_{n,\max}}{\sigma_m+\sigma_R}\right)^2=1 \tag{15}$$

or

$$\sigma_{eq}=\left[\left(\frac{\tau_{\max}}{\tau_m+\tau_R}\right)^2+\left(\frac{\sigma_{n,\max}}{\sigma_m+\sigma_R}\right)^2\right]^{1/2}\sigma_{R=-1} \tag{16}$$

where σ_{eq} is the equivalent fully reversed normal stress. The above equations are valid for proportional loadings. For non-proportional loadings, $\sigma_{n,\max}$ and $\tau_{\max}$ do not occur simultaneously. Generally, for non-proportional loading, a criterion whose expressions change with time is more suitable. Therefore, the corresponding critical plane may be found by a time marching method. Thus, equations such as (3), (4), (9), (10) and (12) that contain stationary parameters, may not seem to be useful for a life assessment under a non-proportional random loading. Furthermore, (3), (4) and (11) suffer from the fact that their results show no difference between the positive and the negative σ_m values. It is an evident that compressive normal stresses, in contrast to the tensive ones, tend to close the crack enclosure and subsequently, enhance the fatigue strength.

J. Sines criterion

Since for non-proportional loadings, $\Delta(\sigma_1-\sigma_2)\neq\Delta\sigma_1-\Delta\sigma_2)$ difficulties arise when calculating $(J_2)_a$. However, in the present research, in contrast to the other references, $\Delta\sqrt{J_2}$ is not computed substituting the principal stresses by their increments in the J_2 expression. $\Delta\sqrt{J_2}$ and $(\sqrt{J_2})_a$ expressions are derived by a time marching procedure in the current paper. Besides, according to the uniaxial fatigue experiments data, it is easily verified that [18]:

$$\alpha=\frac{\sqrt{2}}{3}(\sigma_{R=-1}/\sigma_{R=0}-1)$$
$$\beta=\frac{\sqrt{2}}{3}\sigma_{R=-1} \tag{17}$$

K. Findley criterion

Two limit cases: a hydrostatic stress field situation and a pure torsion loading may be considered to calibrate Findley and McDiarmid criteria. Therefore, one may write:

$$\begin{cases} f=\sqrt{1+k^2}\,\tau_R \\ \psi=\dfrac{k}{\sqrt{1+k^2}}=\dfrac{\tau_R}{(\sigma_k)_{\max R,f}} \end{cases} \tag{18}$$

where $(\sigma_k)_{\max\ R,f}$ is the hydrostatic pressure value corresponding to the fatigue failure at the specified *'R'* value (if it is R-dependent). The function ψ may be determined using experimental data. Therefore, both *'f'* and *'k'* parameters may be considered as functions of *'R'*. Then, using the mean stress correction, one has:

$$\tau_{eq}=\max_{\theta,\varphi,\psi,t}(\tau_R+k\sigma_n)/\sqrt{1+k^2}\,\tau_{R=-1}/\tau_R \tag{19}$$

On the other hand, if the *'f'* parameter is considered as a function that is independent of *'R'*, then, from the uni-axial cyclic loading, one has:

$$\sqrt{\sigma_R^2+k^2(\sigma_m+\sigma_R)^2}+k.(\sigma_m+\sigma_R)=2\sqrt{1+k^2}\,\tau_R$$
$$\Rightarrow\frac{\sigma_{R=0}}{\sigma_{R=-1}}=\frac{k+\sqrt{1+k^2}}{2k+\sqrt{1+4k^2}} \tag{20}$$

This equation can be used to determine the *'k'* parameter.

L. McDiarmid criterion

Using the same limit cases that are mentioned in the previous section, one has:

$$f=(\tau_a)_{AorB}=\tau_R$$
$$(\sigma_a)_{R,f}=2\sigma_u \tag{21}$$

Generally, the second identity does not hold. If we use the function ψ that is defined in (19), we have:

$$\tau_{eq}=[\tau_a+(\sigma_n)_{\max(t)}/\psi].\tau_{R=-1}/\tau_R \tag{22}$$

This equation must be calculated on a plane with maximum shear stress. Using the limit uni-axial cyclic tension case where $\tau_a=\sigma_R/2$ and $\sigma_{n,\max}=(\sigma_m+\sigma_R)/2$ one has:

$$k=\frac{2\tau_R-\sigma_R}{\sigma_m+\sigma_R} \tag{23}$$

If the '*f*' parameter is considered as a function that is independent of '*R*', then, from the uni-axial cyclic tension case, one has:

$$\frac{1+k}{1+2k}=\frac{\sigma_{R=0}}{\sigma_{R=-1}}\Rightarrow k=\frac{\sigma_{R=-1}-\sigma_{R=0}}{2\sigma_{R=0}-\sigma_{R=-1}} \quad (24)$$

M. Carpinteri–Spagnoli theory

Mean stress effect is not included in (9). It is an evidence that when the mean shear stress value of a component reaches the ultimate shear stress value, the component will fail with $(\tau_a=0,\ \sigma_{n,\max(t)}=0)$. Therefore, it seems that (15) is more general than (9).

N. Ninic equation

σ_a and τ_a used in Ninic equation belong to a plane with maximum damage and are different from those parameters appeared in Gough's equation. The '*k*' parameter is extracted from a simple fully reversed uniaxial loading. Ultimate stress values are not considered in the maximization procedure. Besides, there exists noifference between the positive and negative values of σ_m in this formulation. It is proven that the results of Ninic equation are more accurate than the results of the previous mentioned theories [18]. However, the criterion has some limitations.

III. The Proposed Life Assessment Procedure

In the present paper, equivalent stresses are used to predict the components fatigue lives. Miner cumulative damage criterion is used in the present numerical scheme. It is proven that results of Miner's theory for random loadings are more reliable than those obtained for strain-controlled or stress-controlled load cases [14]. The numerical stages are illustrated in compact form in Fig. 4.

In the critical plane approaches proposed so far, the critical plane orientation is considered to be fixed. Cumulative damage that is occurred on this fixed plane is considered to lead to failure. In the present paper, it is assumed that the critical plane orientation vary with time (Fig. 4). Among all planes, one with the greatest cumulative fatigue damage is considered as the critical plane.

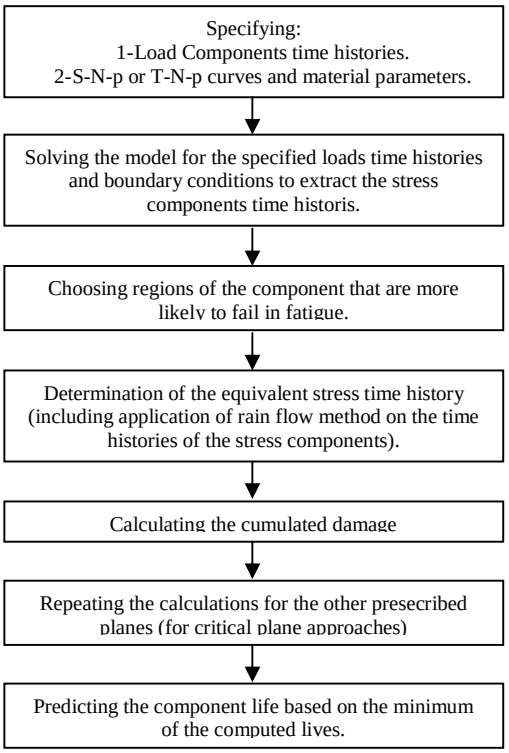

Fig. 4 The proposed numerical life assessment scheme

IV. Inspection of the Fracture

For the analysis of fractured region, a finite element analysis is carried out for the determination of the highly stressed region.

A. Finite element stress analysis

The anti-roll bar is modeled via ANSYS 11/Mechanical module. After the definition of the geometry, the material properties developed by the mentioned experimental studies are entered into the program and a static stress analysis is carried out. Material properties are [15]:

$$\sigma_u=1300Mpa,$$
$$\sigma_{R=-1}=570Mpa,$$
$$\sigma_{R=0}=960Mpa,$$
$$\sigma_{yp}=700Mpa,$$
$$(\tau_a)_{R=-1}=400Mpa,$$
$$(\tau_a)_{R=0}=640Mpa,$$
$$E=206.8Mpa,$$
$$\upsilon=0.3$$

where σ_{yp} is the yield stress of the material.

The corresponding FEM model in ANSYS software environment is illustrated in Fig. 6. Support bushings are modeled using spring elements with six (translational and rotational) stiffness coefficients. Opposite displacements are applied to the ends of the anti-roll bar. The time history of the mentioned displacement input is assumed to be constructed from a repeated block shown in Fig. 6, and the primary subject

of the analysis is to determine the highly stressed region of the cross-section. This determination allows us to assign the beginning point of the fracture.

The finite element mesh is generated with SOLID 95 elements from the element library. This element is a tetrahedron with 20 nodes and 30 degrees of freedom and very sensitive for this type of three-dimensional problems [16, 17]. Smart meshing technique is applied for the mesh generation to allow the program to determine the most appropriate meshing. As a result, the element and node numbers of the solution domain are 18266 and 30514, respectively.

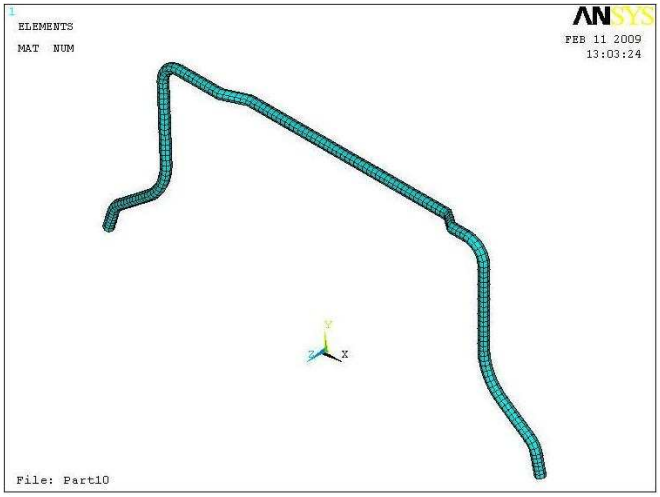

Fig. 5 FEM model of the anti-roll bar

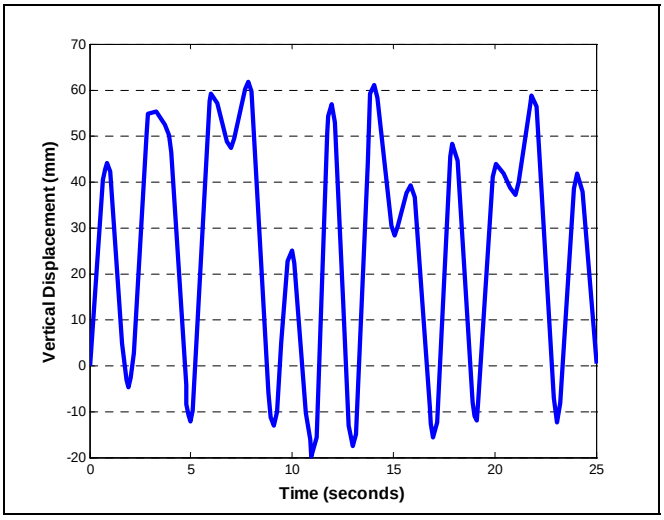

Fig. 6 The second block signal applied on the anti-roll bar component [15]

As a result of the study, the maximum stresses obtained at the third bent location of the bar. To insure that no yielding occurs during loading, so that the fatigue failure occurs in the HCF regime, the effective (Von Mises) stresses of the component are determined based on the greatest stress amplitude of the time history illustrated in Fig. 7. The corresponding results are illustrated in Fig. 7 in Pa. As it may be noticed from Fig. 6, the maximum value of the effective stress is 583 MPa which is greater than $\sigma_{R=-1}$ and less than σ_{yp}. This location is loaded by bending and torsion because of the geometry and boundary conditions. The highest stress is obtained at the inner point of this curved location. The fatigue crack is initiated and propagated from this location.

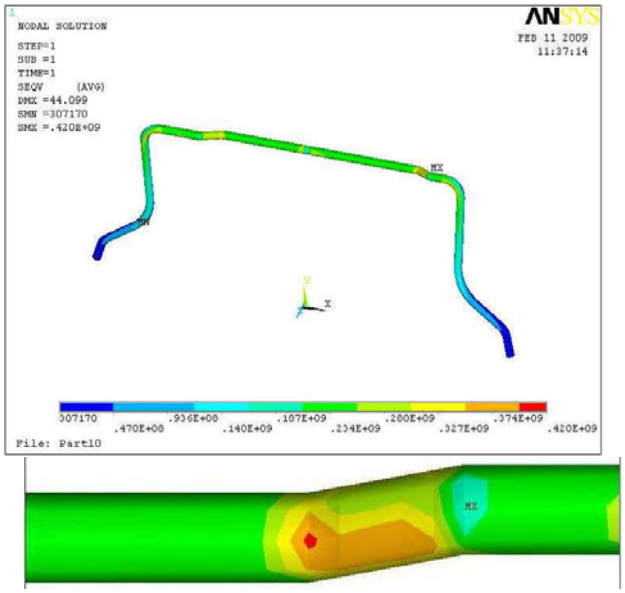

Fig. 7 The effective stresses, based on the greatest stress amplitude of the time history illustrated in Fig. 5

B. Finite element fatigue analysis

Fatigue life assessment of an anti-roll bar component of a passenger vehicle, is investigated. Experimental data reveal that applying opposite fully reversed vertical displacements with amplitude of 50 mm at the ends of the anti-roll bar, will lead to fatigue failure after approximately 49,500 cycles. It has been used the experimental data from reference [18] for validation of FEM results. The FEM model is validated by comparing the static stiffness results obtained from the FEM analysis with the experimental ones. Number of cycles to failure calculated using FEM model via software ANSYS 11 is 55,040 cycles and Number of cycles to failure is calculated using various theories. Results are given in Table I.

To see the mean stress effects, another input is also applied and also number of cycles to failure calculated using FEM model via software ANSYS 11 is 140,870 cycles. As before, the corresponding results are also given in Table I.

For the special cases studied, according to results shown in Table I, modified Sines criterion offers the lowest life values. For fully reversed displacement inputs, the more accurate criteria may be ordered based on the accuracy level as: the general criterion, Gouph and Pollard criterion, Ninic criterion and the modified von Mises theory, respectively. Since more stress components may be considered in the general criterion, lower life is predicted by the general criterion in comparison with Gough–Pollard or Ninic criteria. Significant discrepancies are noticeable in the results of the second type input. Results of von Mises theory are also computed. They are omitted because they were unjustifiably lower than the other results.

For the second type of loading, the more accurate criteria may be ordered based on the accuracy level as: the general criterion, the modified von Mises theory, and the modified Findley criterion, respectively. Remarkable enhancements are noticed due to using the modifications proposed in the present paper. Furthermore, there exist good agreements between the results of the general criterion and the experimental results.

V. Conclusions

In the present paper, as a first stage, some modifications are proposed to some existing fatigue failure models. Many hints that may be considered to develop general fatigue failure models for three-dimensional stress fields with random, non-proportional loadings are mentioned. Then, fatigue life of an anti-roll bar component of a passenger vehicle, is investigated by numerical method and finally comparison is made among the results of the FEM analysis, results of the existing theories, results of the modified versions of the theories, as well as the experimental results. The presented results confirm the accuracy of numerical fatigue analysis.

TABLE I
Comparisons among the results of the existing theories, results of the modified or proposed criteria, and the experimental results

Result Title	Fully reversed input	Input shown in Fig.5
This study (ANSYS)	55,040	140,870
Experimental [18]	49,500	116,820
Gough-Pollard	70,301	328,371
Modified sines	23,275	58,901
Fidley	90,146	280,892
McDiarmid	91,713	296,172
Carpinteri-Spagnoli	76,799	276,855
Ninic	70,301	213,673
Modified Fidley	82,614	196,563
Modified McDiarmid	78,346	226,389
Modified Von Mises	81,713	186,407
The general criterion	67,168	162,623

References

[1] H. Heisler, "Vehicle and engine technology," 2nd ed. London: SAE International, 1999.
[2] TD. Gillespie, "Fundamentals of vehicle dynamics," SAE Publication, 1992.
[3] A. Fatemi, L. Yang, "Cumulative fatigue damage and life prediction theories: a survey of the state of the art for homogeneous materials," Int J Fatigue, vol. 20, no. 1, pp. 9–34, 1998.
[4] P. Haupt, "Continuum mechanics and theory of materials," Springer-Verlag, 2002.
[5] G. Sines, "Behavior of metals under complex stresses," In Metal fatigue, G. Sines, JL. Waisman, Ed. New York: McGraw-Hill, 1959.
[6] YC. Fung, P. Tong, "Classical and computational solid mechanics," World Scientific Publishing Co. Inc., 2001.
[7] WN. Findley, "A theory for effect of mean stress on fatigue of metals under combined torsion and axial load or bending," J Eng Ind, pp. 301–6, 1959.
[8] MW. Brown, KJ. Miller, "A theory for fatigue failure under multiaxial stress–strain conditions," Proc Inst Mech Eng, vol. 187, no. 65, pp. 745–55, 1973.
[9] A. Carpinteri, R. Brighenti, and A. Spagnoli, "A fracture plane approach in multiaxial high-cycle fatigue of metals," Fatigue Fract Eng Mater Struct, vol. 23, no. 4, pp. 355–64, 2000.
[10] A. Carpinteri, A. Spagnoli, "Multiaxial high-cycle fatigue criterion for hard metals," Int J Fatigue,vol. 23, pp. 135–45, 2001.
[11] A. Spagnoli, "A new high-cycle fatigue criterion applied to out-ofphase biaxial stress state," Int J Mech Sci, vol. 43, pp. 2581–95, 2001.
[12] HJ. Gough, HV. Pollard, "The strength of metals under combined alternating stresses," Proc Inst Mech Eng, vol. 131, pp. 1–103, 1935.
[13] Y. Liu, S. Mahadevan, "A unified multiaxial fatigue damage model for isotropic and anisotropic materials," Int J Fatigue,vol. 29, pp. 347–59, 2007.
[14] DH. Wright, "Testing automotive materials and components," McGraw-Hill Publishing Co., 1993.
[15] M. Shariyat, "A fatigue model developed by modification of Gough's theory, for andom non-proportional loading conditions and three-dimensional stress fields," Int J Fatigue, vol. 30, pp. 1248–1258, 2008.
[16] J. Schijve, "Fatigue of structures and materials," Secaucus, (NJ, USA): Kluwer Academic Publishers, 2001.
[17] ANSYS 5.4 versions users manual.
[18] M. Shariyat, A. Ganjidoust, "Fatigue failure and damage analysis of an anti-roll bar under random fatigue tests," Journal of Solid Mechanics, pp. 3–20, 2010.

Javad Marzbanrad is an associate professor in Automotive Engineering at Iran University of Science and Technology. He was born in 1964 in Tehran, Iran. He got his Ph.D's Degree in 2001 from Tarbiat Modarres University. He was in the Clarkson University, NY, U.S. in 2000-01 as visiting scholar. His research interests are Automotive, Control and Vibration and Solid Mechanics. Now, he is the faculty of School of Automotive Engineering in Iran University of Science and Technology. He has more than 150 published papers in the conferences and journals. He also published three books in mechanical software fields. He has also registered six inventions in Iran.

Aref Yadollahi was born in 1984 in Semnan, Iran. He got his MSc's Degree in 2010 from Iran University of Science and Technology. His research interests are Automotive, NVH and Solid Mechanics. Now, he is the tutor of Automotive Department in the Islamic Azad University, Semnan Branch. He has more than 10 published papers in the conferences and journals. He also published one book in mechanical software field.